Robust ℓ_∞-Stability of Systems with Repeated Perturbations: A Case Study

PATRICK CADOTTE[1], HANNAH MICHALSKA[2], BENOIT BOULET[3]
Centre for Intelligent Machines
McGill University
3480 University Street, Montreal, H3A 2A7
CANADA

Abstract: - The paper presents a pair of necessary and sufficient conditions for robust ℓ_∞-stability of discrete-time systems with structured, repeated, linear time-varying, induced ℓ_∞-norm bounded perturbations. The quality of these conditions is confirmed employing a realistic example involving an electronic circuit with repeated operational-amplifiers, persistent noise disturbances, and peak-to-peak gain performance objectives.

Key-Words: - Robust Control, ℓ_∞-Stability, Repeated Perturbations, Linear Systems, Optimization

1 Introduction

Robust ℓ_p-stability problems are usually re-stated as satisficing problems involving the computation of a structured norm; see §3 for a definition of the structured norm and see [6] for a comprehensive summary of relevant results and references. However, in general, the exact computation of the structured norm is a very difficult task. It is hence customary to substitute the structured norm by its upper bound approximation as derived from the scaled small gain theorem. The level of conservativeness of such upper bound depends on the nature of the robust stability problem, more precisely, the class of perturbations considered.

In the particular case when the perturbations are structured, independent (i.e., not repeated), linear time-varying (LTV), and induced ℓ_∞-norm bounded, it was shown by Khammash&Pearson, [11], that the abovementioned upper bound is indeed equal to the structured norm value itself. Similar results derived later, see Shamma, [15], and Young&Dahleh, [16], extend these results to the induced ℓ_2-norm bounded problem and to the general induced ℓ_p-norm bounded problem, respectively.

Since systems with repeated components appear often in practical applications, see [2], the class of robust stability problems with repeated perturbations certainly deserves more attention. Unfortunately, the above results fail to hold for structured, *repeated*, LTV, induced ℓ_∞-norm bounded perturbations which motivates the developments of the present paper where new necessary and sufficient conditions for the stability of such systems are derived. The new sufficient stability condition is derived from the implementation of a particular type of system augmentation within the scaled small gain theorem. The result is conceptually simple, yet it permits a significant decrease in the conservativeness of design and analysis in many robustness problems as compared with previous techniques, see [3] and [4]. On the other hand, the new necessary condition allows to assess the tightness of the proposed sufficient condition and to identify ineffective (i.e., non-robust) designs, see [1].

The derived results are applied to a practical robust ℓ_∞-performance problem involving an electronic circuit with repeated operational-amplifiers, persistent noise disturbances, and peak-to-peak gain performance objectives. The numerical and experimental results obtained confirm the efficiency of the proposed approach.

The paper is structured as follows. The required notation is introduced in §2. Then, the robustness problem is stated in §3, followed by the corresponding sufficient and necessary conditions for stability in §4 and §5, respectively. Finally, the theoretical results are applied to a realistic example in §6.

2 Notation

Let $0_{m\times n}$ and I_n denote the zero matrix of dimension $m\times n$ and the identity matrix of dimension $n\times n$, respectively. For any matrix $A \in \mathbb{R}^{m\times n}$, $A \triangleq [A_{ij}]_{\substack{i\in\{1,\dots,m\}\\ j\in\{1,\dots,n\}}}$, where A_{ij} is the ij^{th} entry of A. Similarly, for any vector $a \in \mathbb{R}^n$, $a \triangleq [a_1 \dots a_n]^T$, where a_i is the i^{th} entry of a. This notation carries to the case of MIMO systems and vector signals. Let A^T and $\rho(A)$ denote the transpose and the spectral radius of the matrix A, re-

spectively. Given a matrix $A \in \mathbb{R}^{m\times n}$, define

$$\mathrm{sgn}(A) \triangleq [\mathrm{sgn}(A_{ij})]_{\substack{i\in\{1,\dots,m\}\\ j\in\{1,\dots,n\}}},$$

where $\mathrm{sgn}(A_{ij}) \triangleq \begin{cases} +1 & \text{if} \quad A_{ij} \geq 0 \\ -1 & \text{if} \quad A_{ij} < 0 \end{cases}$.

Consider the system P partitioned as follows $P \triangleq \begin{bmatrix} P^{11} & P^{12} \\ P^{21} & P^{22} \end{bmatrix}$. Given the system Q of dimension compatible with P^{22}, let

$$F_l(P,Q) \triangleq P^{11} + P^{12}Q(I - P^{22}Q)^{-1}P^{21}$$

denote the lower linear fractional transformation between P and Q. Similarly, given the system R of dimension compatible with P^{11}, let

$$F_u(P,R) \triangleq P^{22} + P^{21}R(I - P^{11}R)^{-1}P^{12}$$

denote the upper linear fractional transformation between P and R.

Let ℓ_p^n denote the space of all infinite sequences $\{s(k)\}_{k=0}^{\infty}$ of vectors of lenght n, $s(k) \in \mathbb{R}^n$, equipped with the norm $\|s\|_p < \infty$, where

$$\|s\|_p \triangleq \sqrt[p]{\sum_{k=0}^{\infty}\sum_{i=0}^{n}|s_i(k)|^p}.$$

For $p = \infty$, also define $\|s\|_\infty \triangleq \sup_{k\geq 0}\max_{i\in\{1,\dots,n\}}|s_i(k)|$. Given a bounded operator $S : \ell_p^n \mapsto \ell_p^m$ with $s \mapsto S(s)$, let

$$\|S\|_{p-ind} \triangleq \sup_{s\neq 0}\frac{\|S(s)\|_p}{\|s\|_p}$$

be the induced p-norm of S. Furthermore, if S is linear and causal, then $S(s)$ is determined by the convolution $(S * s)(k) \triangleq \sum_{l=0}^{k} S(k,l)s(l)$, where $S(k,l)$ denotes the kernel of S. In the case when S is also time-invariant, $S(s)$ simplifies to $(S * s)(k) \triangleq \sum_{l=0}^{k} S(l)s(k-l)$, where $\{S(l)\}_{l=0}^{\infty}$ is the impulse response of S. Then, it is known that, see [6], $\|S\|_{\infty-ind} = \|S\|_1$, where

$$\|S\|_1 \triangleq \max_{i\in\{1,\dots,m\}}\sum_{j=1}^{n}\sum_{k=0}^{\infty}|S_{ij}(k)|. \qquad (1)$$

3 Problem Statement

Let the set $\mathbf{\Delta}$ denote a given class of admissible perturbations which carries all the important information relevant to the nature and structure of the perturbations. Assume that $\Delta \in \mathbf{\Delta}$ and that M is a system of dimension compatible with Δ, as illustrated by Fig.1. The structured norm of M is then defined as:

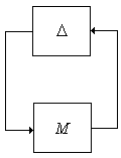

Fig. 1: The $M\Delta$-loop.

$$SN_{\mathbf{\Delta},p}(M) \triangleq \frac{1}{\inf_{\Delta\in\mathbf{\Delta}}\{\|\Delta\|_{p-ind} : (I-M\Delta)^{-1} \text{ is not } \ell_p\text{-stable}\}}.$$

If for every $\Delta \in \mathbf{\Delta}$, $(I - M\Delta)^{-1}$ remains ℓ_p-stable, then it is assumed that $SN_{\mathbf{\Delta},p}(M) = 0$. Recall that, the structured norm is not a norm, see [6].

Furthermore, assuming that $\|\Delta\|_{p-ind} < 1$, it is seen that robust ℓ_p-stability of the $M\Delta$-loop is equivalent to the condition: $SN_{\mathbf{\Delta},p}(M) \leq 1$. However, in general, it is not possible to compute $SN_{\mathbf{\Delta},p}(M)$ exactly due to the complexity of such a task. Practical approaches hence rely on the derivation of upper and lower bounds for $SN_{\mathbf{\Delta},p}(M)$ that can be computed with relative ease, but at the cost of introducing some conservativess.

Given an integer $n \in \mathbb{Z}^+$ together with n integers $p_I \in \mathbb{Z}^+$, $I \in \{1,...,n\}$, define the following classes of perturbations:

$$\begin{aligned} &\mathbf{\Delta}_{LTV}^{1\times 1} \triangleq \{\Delta : \Delta \text{ is SISO, causal, and LTV}\}, \\ &\mathbf{\Delta}^{rep} \triangleq \{\mathrm{diag}(\delta_I I_{p_I}) : \delta_I \in \mathbf{\Delta}_{LTV}^{1\times 1}, I \in \{1,...,n\}\}. \end{aligned} \qquad (2)$$

In the degenerate case where $p_I = 1$ for every $I \in \{1,...,n\}$, $\mathbf{\Delta}^{rep}$ is sometimes refered to as $\mathbf{\Delta}^{ind}$.

Problem Statement: Let M be a discrete, causal, stable, linear time-invariant (LTI) system characterized by the impulse response $\{M(k)\}_{k=0}^{\infty}$ and of dimension compatible with $\Delta \in \mathbf{\Delta}^{rep}$, $\|\Delta\|_{\infty-ind} < 1$, as illustrated by Fig.1. The problem is to ascertain robust ℓ_∞-stability of the $M\Delta$-loop, i.e., find conditions which allow to determine whether $SN_{\mathbf{\Delta}^{rep},\infty}(M) \leq 1$ or $SN_{\mathbf{\Delta}^{rep},\infty}(M) > 1$.

Proposed Solution: The above Problem Statement requires the computation of the structured norm $SN_{\mathbf{\Delta}^{rep},\infty}(M)$. As pointed out, a practical solution is to develop necessary and sufficient conditions for robust ℓ_∞-stability of the $M\Delta$-loop in terms of upper and lower bounds for $SN_{\mathbf{\Delta}^{rep},\infty}(M)$.

The following partitioning of M (partitioning which closely corresponds to that of the set $\mathbf{\Delta}^{rep}$) will be used extensively throughout this paper. Let $q \triangleq \sum_{I=1}^{n} p_I$ and define

$$M \triangleq \left[M^{IJ}\right]_{\substack{I\in\{1,\ldots,n\}\\ J\in\{1,\ldots,n\}}}, \tag{3}$$

where $M^{IJ} \triangleq \left[M_{ij}^{IJ}\right]_{\substack{i\in\{1,\ldots,p_I\}\\ j\in\{1,\ldots,p_J\}}}$. Note that M has q inputs and q outputs, while M^{IJ} has p_J inputs and p_I outputs. The above partitioning of M induces a corresponding partitioning of its impulse response.

4 A Sufficient Condition for Robust ℓ_∞-Stability

A sufficient condition for robust ℓ_∞-stability of the $M\Delta$-loop of the Problem Statement is presented next. An associated upper bound for the structured norm $SN_{\mathbf{\Delta}^{rep},\infty}(M)$ is also derived.

The following notation is used in the sequel.

Given a sequence

$$\mathbf{a} \triangleq \{a_1, ..., a_I, ..., a_n\}, \tag{4}$$

where $a_I \in \mathbb{Z}^+$, and a system M partitioned according to (3), define the augmented system

$$M_{\mathbf{a}} \triangleq \begin{bmatrix} M^{11} & 0_{p_1\times a_1} & \ldots & M^{1n} & 0_{p_1\times a_n} \\ 0_{a_1\times p_1} & 0_{a_1\times a_1} & \ldots & 0_{a_1\times p_n} & 0_{a_n\times a_n} \\ \vdots & \vdots & \ddots & \vdots & \vdots \\ M^{n1} & 0_{p_n\times a_1} & \ldots & M^{nn} & 0_{p_n\times a_n} \\ 0_{a_n\times p_1} & 0_{a_n\times a_1} & \ldots & 0_{a_n\times p_n} & 0_{a_n\times a_n} \end{bmatrix}.$$

Theorem 4.1 *Let M be a discrete, causal, stable, LTI system of dimension compatible with $\Delta \in \mathbf{\Delta}^{rep}$, $\|\Delta\|_{\infty-ind} < 1$, as illustrated by Fig.1. Given any sequence $\mathbf{a}$, as in (4), if there exists a $D \in \mathbf{D}_{\mathbf{a}}^{rep}$ such that*

$$\|D^{-1}M_{\mathbf{a}}D\|_1 \leq 1, \tag{5}$$

where

$$\mathbf{D}_{\mathbf{a}}^{rep} \triangleq \{\mathrm{diag}(D^I) : D^I \in \mathbb{R}^{(p_I+a_I)\times(p_I+a_I)}, D^1_{11} = 1, D^I_{11} \geq ... \geq D^I_{1(p_I+a_I)} \geq 0, I \in \{1, ..., n\}\}, \tag{6}$$

then the $M\Delta$-loop is robustly ℓ_∞-stable.

Proof: See [4] for a detailed proof.

Corollary 4.2 *Consider the system of Theorem 4.1. For any given $\mathbf{a}$, as in (4), the optimization problem*

$$\overline{SN}_{\mathbf{D}_{\mathbf{a}}^{rep},\infty}(M) \triangleq \min_{D\in\mathbf{D}_{\mathbf{a}}^{rep}} \|D^{-1}M_{\mathbf{a}}D\|_1 \tag{7}$$

yields an upper bound for the structured norm of M, i.e., $\overline{SN}_{\mathbf{D}_{\mathbf{a}}^{rep},\infty}(M) \geq SN_{\mathbf{\Delta}^{rep},\infty}(M)$.

Condition (5) is referred to as the *standard sufficient condition* when $\mathbf{a} = \{0, ..., 0\}$ and as the *augmented sufficient condition* when $\mathbf{a}$ contains positive elements. Note that robust stability conditions similar to the standard sufficient condition are widely employed in the control literature, while the augmented sufficient condition has only been proposed very recently in [4]. It is clear from the definitions of $\mathbf{D}_{\mathbf{a}}^{rep}$ and $M_{\mathbf{a}}$ that the augmented sufficient condition implies the standard one. Yet, it was shown in [4], that the augmented sufficient condition often leads to less conservative stability conditions then its standard counterpart.

5 A Necessary Condition for Robust ℓ_∞-Stability

A necessary condition for robust ℓ_∞-stability of the $M\Delta$-loop of the Problem Statement is presented next. An associated lower bound for the structured norm $SN_{\mathbf{\Delta}^{rep},\infty}(M)$ is also derived.

The following notation is used in the sequel.

The class of admissible collections of subsets is defined by

$$\mathbf{\Upsilon} \triangleq \{\Upsilon : \Upsilon = \{\mathbf{\Gamma}(\kappa)\}_{\kappa=0}^{\upsilon-1}, \mathbf{\Gamma}(\kappa) \subseteq \mathbb{Z}^*, \mathbf{\Gamma}(\kappa) \neq \emptyset, \bigcap_{\kappa=0}^{\upsilon-1} \mathbf{\Gamma}(\kappa) = \emptyset, \upsilon \in \mathbb{Z}^*\}.$$

Note that each $\Upsilon \in \mathbf{\Upsilon}$ is a collection of distinct subsets of $\mathbb{Z}^*$. Define

$$\mathbf{Y} \triangleq \{\Upsilon^{IJ}\}_{\substack{I\in\{1,\ldots,n\}\\ J\in\{1,\ldots,n\}}}, \tag{8}$$

where $\Upsilon^{IJ} = \{\mathbf{\Gamma}^{IJ}(\kappa)\}_{\kappa=0}^{\upsilon_{IJ}-1} \in \mathbf{\Upsilon}$, and

$$\mathbf{N} \triangleq \{N_I\}_{I\in\{1,\ldots,n\}}, \tag{9}$$

where $N_I \in \mathbb{Z}^+$.

For the above fixed $n \in \mathbb{Z}^+$, $\upsilon_{IJ} \in \mathbb{Z}^+$, and $N_I \in \mathbb{Z}^+$, where $I, J \in \{1, ..., n\}$, define the set of indices

$$\mathbf{x} \triangleq \{(\kappa, \imath, \jmath, I, J) : \kappa \in \{0, ..., \upsilon_{IJ} - 1\}, \imath \in \{1, ..., N_I\}, \jmath \in \{1, ..., N_J\}, I \in \{1, ..., n\}, J \in \{1, ..., n\}\}$$

and the class of admissible sets of real numbers

$$\mathbf{d} \triangleq \{d = \{d_{\imath\jmath}^{IJ}(\kappa)\}_{(\kappa,\imath,\jmath,I,J)\in\mathbf{x}} : d_{\imath\jmath}^{IJ}(\kappa) \in \mathbb{R}\}. \tag{10}$$

Theorem 5.1 *Let M be a discrete, causal, stable, LTI system characterized by an impulse response $\{M(k)\}_{k=0}^{\infty}$, partitioned as in (3), and of dimension compatible with $\Delta \in \mathbf{\Delta}^{rep}$, $\|\Delta\|_{\infty-ind} < 1$, as illustrated by Fig.1. For given $\mathbf{N}$ and $\mathbf{Y}$ (as defined by (9) and (8)), if there exists a set of real numbers $d \in \mathbf{d}$ satisfying:*

$$i)\ \ \rho\left(\Xi(d)\right) > 1 \tag{11}$$

where $\Xi(d) \triangleq \left[\xi^{IJ}\right]_{\substack{I\in\{1,\dots,n\}\\ J\in\{1,\dots,n\}}}$, $\xi^{IJ} \triangleq \left[\xi_{\imath\jmath}^{IJ}\right]_{\substack{\imath\in\{1,\dots,N_I\}\\ \jmath\in\{1,\dots,N_J\}}}$, $\xi_{\imath\jmath}^{IJ} \triangleq \sum_{\kappa=0}^{\upsilon_{IJ}-1}\left(d_{\imath\jmath}^{IJ}(\kappa) \sum_{k\in\mathbf{\Gamma}^{IJ}(\kappa)} M^{IJ}(k)\right)$, *and*

$$ii)\ \ \max\Big\{\sum_{\jmath=1}^{N_J}|d_{\imath\jmath}^{IJ}(\kappa)| : \kappa\in\{0,...,\upsilon_{IJ}-1\}, \tag{12}$$
$$I\in\{1,...,n\}, J\in\{1,...,n\}, \imath\in\{1,...,N_I\}\Big\} < 1,$$

then the $M\Delta$-loop fails to be robustly ℓ_∞-stable.

Proof: See [1] for a detailed proof.

Corollary 5.2 *Consider the system of Theorem 5.1. For any given $\mathbf{N}$ and $\mathbf{Y}$, the optimization problem*

$$\underline{SN}_{\mathbf{Y},\mathbf{N},\infty}(M) \triangleq \max_{d\in\mathbf{d}}\{\rho\left(\Xi(d)\right) : (12) \text{ holds}\} \tag{13}$$

yields a lower bound for the structured norm of M, i.e., $\underline{SN}_{\mathbf{Y},\mathbf{N},\infty}(M) \le SN_{\mathbf{\Delta}^{rep},\infty}(M)$.

Detailed guidelines for the choice of $\mathbf{N}$ and $\mathbf{Y}$ are given in [1]. In particular, the following rules and definitions will prove to be helpful in the context of the practical application presented in §6.

Consider the $M\Delta$-loop as defined in the Problem Statement. Without loss of generality, it is shown in [1] that it is always possible to rearrange the impulse response of M so that

$$M_{11}^{IJ}(k) \ge 0 \tag{14}$$

for every $I \in \{1,...,n\}$, $J \in \{1,...,n\}$, and $k \in \mathbb{Z}^*$. Moreover, if for a given I, $p_I = 1$ (i.e. I corresponds to a perturbation block which is not repeated), then $\underline{SN}_{\mathbf{Y},\mathbf{N},\infty}(M)$ achieves its maximal value with respect to N_I at $N_I = 1$.

Corresponding to the impulse response of M, define

$$\Upsilon_S^{IJ} \triangleq \{\mathbf{\Gamma}_S^{IJ}(\kappa)\}_{\kappa=0}^{\upsilon-1},$$

where $\mathbf{\Gamma}_S^{IJ}(\kappa) \triangleq \Big\{\Gamma \in \mathbb{Z}^* : M^{IJ}(\Gamma) = \alpha_\Gamma M^{IJ}(\bar\kappa), \alpha_\Gamma \in \mathbb{R}, \bar\kappa = \min\{k\in\mathbb{Z}^* : k \notin \bigcup_{\bar k=0}^{\kappa-1}\mathbf{\Gamma}_S^{IJ}(\bar k)\}\Big\}$. The subsets of indices of the form $\mathbf{\Gamma}_S^{IJ}(\kappa)$ capture any possible linear dependence between any two matrices of the form $M^{IJ}(k)$, $k \in \mathbb{Z}^*$. Similarly, let

$$\Upsilon_\pm^{IJ} \triangleq \{\mathbf{\Gamma}_\pm^{IJ}(\kappa)\}_{\kappa=0}^{\upsilon-1}$$

where $\mathbf{\Gamma}_\pm^{IJ}(\kappa) \triangleq \Big\{\Gamma \in \mathbb{Z}^* : \text{sgn}\left(M^{IJ}(\Gamma)\right) = \text{sgn}\left(M^{IJ}(\bar\kappa)\right), \bar\kappa = \min\{k\in\mathbb{Z}^* : k \notin \bigcup_{\bar k=0}^{\kappa-1}\mathbf{\Gamma}_\pm^{IJ}(\bar k)\}\Big\}$. The subsets of indices of the form $\mathbf{\Gamma}_\pm^{IJ}(\kappa)$ capture the similarities between the distributions of nonnegative entries in each $M^{IJ}(k)$, $k \in \mathbb{Z}^*$. Note that $\Upsilon_\pm^{IJ}, \Upsilon_S^{IJ} \in \mathbf{\Upsilon}$.

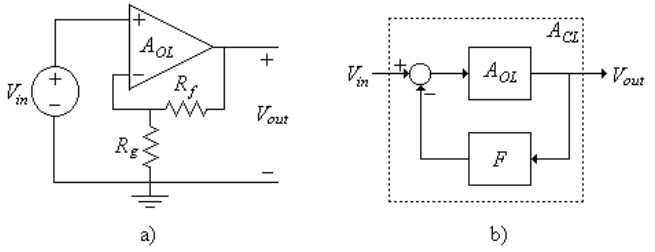

Fig. 2: The op-amp non-inverting configuration and its equivalent mathematical model. Symbols used: V_{in} and V_{out} are the input and output voltage signals, respectively; R_f and R_g are the feedback and the grounded resistors, respectively; the blocks A_{OL} and A_{CL} describe the open-loop and closed-loop op-amp dynamics, respectively; F denotes the feedback gain.

6 Application to Electronic Circuits

The theoretical developments of the previous sections will be applied to study robust ℓ_∞-stability of an electronic circuit system comprising a pair of operational-amplifiers (op-amps) and affected by exogenous noise disturbances.

The electronic circuit system is described below in terms of its mathematical model which captures the main physical characteristics, operating conditions, and performance objectives relevant to this circuit. Necessary and sufficient robust ℓ_∞-stability conditions are then derived based on Theorem 4.1 and Theorem 5.1. These conditions are subsequently compared with experimental results (obtained using a harware circuit simulator) to further assess their quality.

6.1 The Non-Inverting Op-Amp Configuration

Consider the set-up depicted in Fig.2. Fig.2a shows an op-amp in standard non-inverting configuration, while Fig.2b presents its equivalent mathematical model. The closed-loop transfer function of this non-inverting configuration is given by

$$A_{CL} \triangleq \frac{V_{out}}{V_{in}} = \frac{A_{OL}}{1 + A_{OL}F},$$

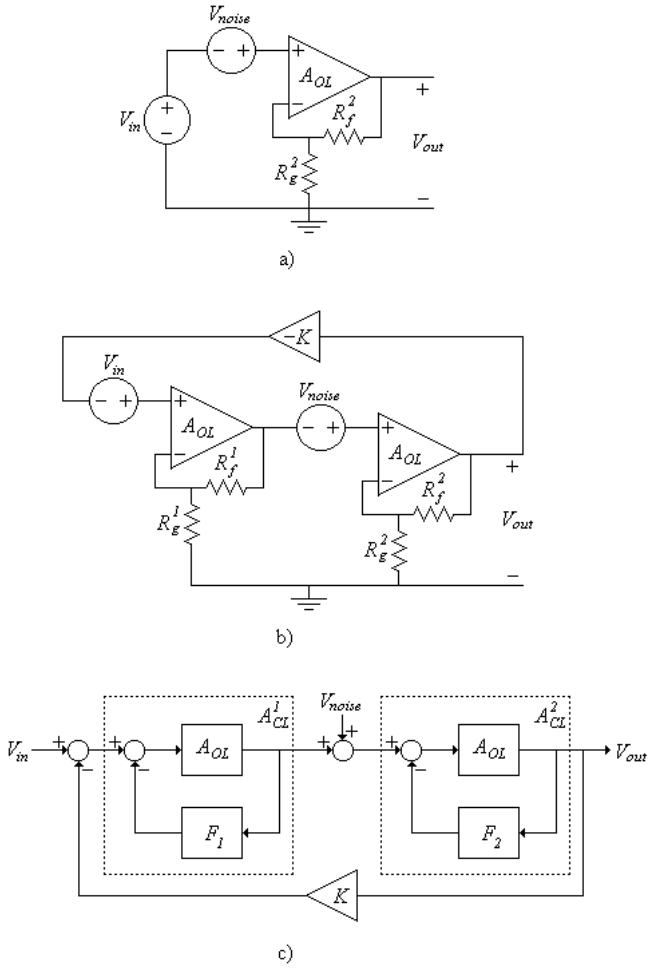

Fig. 3: The original noisy circuit, the corresponding noise reduction circuit, and the equivalent mathematical model of the noise reduction circuit. Symbols used: V_{in}, V_{out}, and V_{noise} are the input, output, and noise voltage signals, respectively; (R_f^1, R_g^1) and (R_f^2, R_g^2) are the first and second stage pairs of resistors, respectively; the blocks A_{OL}, A_{CL}^1 and A_{CL}^2 describe the open-loop, first stage closed-loop, and second stage closed-loop op-amp dynamics, respectively; F_1, F_2, and K denote the first and second stage feedback gains and the proportional controller, respectively.

where $F \triangleq \frac{R_g}{(R_g+R_f)}$. For the ideal case where $A_{OL} = \infty$,

$$A_{CL} = 1 + \frac{R_f}{R_g}. \tag{15}$$

6.2 Noise Reduction Problem

The noise reduction problem adressed in this paper is also discussed in [14] as it is relatively common in practice. Consider the situation illustrated in Fig.3. Fig.3a shows an electronic circuit with a pair of input and output signals interconnected by a single amplifier stage subjected to noise. It is assumed that the noise disturbance signal V_{noise} enters at the input of the op-amp. The objective is to find a way to reduce the overall influence of this noise on the electronic circuit. In Fig.3b, an additional (noise free) amplifier stage is introduced, preprocessing the input signal to the noisy amplifier stage. A negative proportional feedback controller closes the loop between the input and output of this system. Provided that the values of R_f^1, R_g^1 and K are suitably chosen, the proposed circuit of Fig.3b allows to reduce significantly the influence of V_{noise} under minimal change of the input-output transfer function $\frac{V_{out}}{V_{in}}$ as displayed by the original circuit of Fig.3a; see [14] for a detailed explanation.

To acquire some insight into how the values of R_f^1, R_g^1 and K can be selected, it is customary to assume that the op-amps used are ideal, i.e., $A_{OL} = \infty$. From Fig.3c and equation (15), it follows that

$$A_{CL}^i \triangleq 1 + \frac{R_f^i}{R_g^i}, \tag{16}$$

where $i \in \{1, 2\}$. By principle of superposition,

$$V_{out} = \frac{A_{CL}^1 A_{CL}^2}{1 + A_{CL}^1 A_{CL}^2 K} V_{in} + \frac{A_{CL}^2}{1 + A_{CL}^1 A_{CL}^2 K} V_{noise}.$$

In this context, the noise versus input reduction ratio is given by

$$\frac{V_{noise}}{V_{in}} = \frac{1}{A_{CL}^1}. \tag{17}$$

Additionally, if it is desired to maintain the same ratio $\frac{V_{out}}{V_{in}} = A_{CL}^2$ in both circuits depicted in Figs.3a and 3b, then the value of the controller gain K must be

$$K = \frac{A_{CL}^1 - 1}{A_{CL}^1 A_{CL}^2}. \tag{18}$$

Equations (17) and (18) suggest that the optimal way to eliminate the undesirable influence of V_{noise}, while preserving the ratio $\frac{V_{out}}{V_{in}}$, is to increase the gain of A_{CL}^1 as much as possible and adjust K accordingly. Such an approach is sufficient only under the additional assumption that both V_{in} and V_{noise} are signals containing relatively low frequency components. Therefore, any low frequency disturbance issue, such as a DC offset, would be efficiently attenuated. While the frequency characteristics of V_{in} can be restricted to low pass, the same does not hold for V_{noise} which typically exhibits a large bandwith. As a result, since A_{OL} is never ideal in practice, a blind application of the above strategy may result in undesirable transient behaviours, e.g., large overshoot spikes in the output signal V_{out}. In these circumstances, the theory proposed in §3 to §5, in conjunction

with (17) and (18), offer a possibility to achieve a reasonable trade-off between a desirable low frequency ratio $\frac{V_{noise}}{V_{in}}$ and an admissible peak-to-peak gain in $\frac{V_{out}}{V_{noise}}$ for the real op-amps circuit of Fig.3b.

6.3 Performance Objectives and Operating Conditions

To appreciate the usefulness of the results presented in §3, §4, and §5, six different noise reduction parameter settings are studied towards assessing the quality of their respective system transient response in terms of peak-to-peak gain. These settings are derived directly from (16)–(18) and are displayed in Table 1. Note that the gain K increases from zero (open-loop case) to one as the noise reduction ratio $\frac{V_{noise}}{V_{in}}$ decreases from 0dB to -100dB (almost complete noise attenuation case).

It is also assumed that V_{noise} is a persistent signal bounded in magnitude by ± 10mV. The critical performance objective is that V_{out} remains within ± 15mV (i.e., $V_{out} \leq 150\% \|V_{noise}\|_\infty$) when $V_{in} = 0$mV. The input signal V_{in} is set here to 0mV for the purpose of the robust analysis, but it is reasonable to assume that any input signals whose variations are restricted to the interval ± 200mV may be significantly affected by the noise signal considered.

6.4 A Linear Model of the Circuit

The op-amps considered here are two identical $\mu 741$ chips. Considering the above operating conditions, a linear model of the open-loop dynamic of the $\mu 741$, derived from Fairchild's $\mu 741$ data sheet, see [7], and validated with PSpice freeware version, see [13], is given below

$$A_{OL}^{\mu 741} \triangleq A(s) + W_\Delta(s)\Delta_A, \tag{19}$$

with $A(s) \triangleq g_A \frac{2\pi f_A}{s+2\pi f_A}$, $W_\Delta \triangleq g_\Delta \frac{s+0.01}{s+2\pi f_\Delta}$, $\Delta_A \in \mathbf{\Delta}_{LTV}^{1\times 1}$, $\|\Delta_A\|_{\infty-ind} < 1$, where $g_A = 1.7 \times 10^5$, $f_A = 9.5$Hz, $g_\Delta = 0.1$, and $f_\Delta = 50$kHz. As explained in [6], the term $W_\Delta(s)\Delta_A$ (with $\Delta_A \in \mathbf{\Delta}_{LTV}^{1\times 1}$ and $\|\Delta_A\|_{\infty-ind} < 1$) including a perturbation block and a high-pass filter, should be large enough to include any possible unmodelled high frequency dynamics as well as potential variations in temperature and power supply that are known to alter the op-amp behaviour. According to [8], temperature and voltage supply fluctuations are considered the most important external sources of dynamic perturbations, but these are not critical here as the temperature and voltage supply are kept constant at 27^oC and 12V, respectively.The above choice of operating conditions also prevents any op-amp saturation issues.

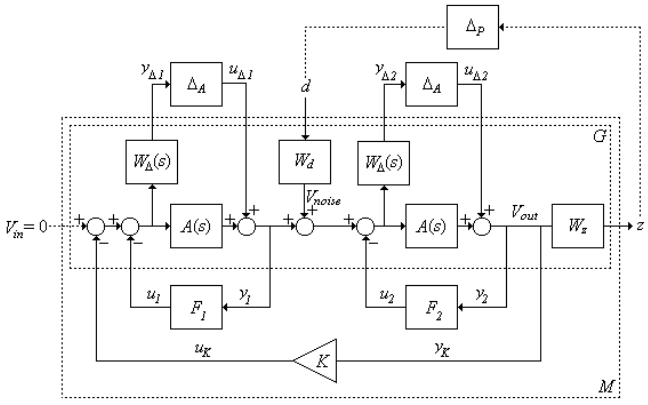

Fig. 4: Typical robust performance block diagram for the noise reduction circuit. Symbols used: d and z are the disturbance and performance signals, respectively; (u_1,y_1), (u_2,y_2), and (u_K,y_K), are pairs of command and measured signals for the first stage, second stage, and controller, respectively; ($u_{\Delta 1}$,$y_{\Delta 1}$) and ($u_{\Delta 2}$,$y_{\Delta 2}$) are pairs of output and input signals for the first and second stage perturbations, respectively; V_{in}, V_{out}, and V_{noise} are the input, output, and noise voltage signals, respectively; the blocks $A(s)$, F_1, F_2, and K describe the op-amp linear approximation of the open-loop dynamic, the first and second stage feedback gains, and the controller, respectively; Δ_A and Δ_P denote the op-amp and performance perturbation blocks, respectively; the block W_d, W_z, and $W_\Delta(s)$ describe the disturbance, performance, and op-amp perturbation weights, respectively; G denotes the augmented plant; M denotes the system to be investigated in an $M\Delta$-loop as proposed in the Problem Statement.

The electronic circuit system of Figs.3b and 3c is further represented in the form of the block diagram shown in Fig.4 to include (19) as well as the weighting functions $W_d = 0.01$ and $W_z = \frac{1}{0.015}$. The weights W_d and W_z correspond to V_{noise} being bounded in magnitude by 10mV and to V_{out} remaining within ± 15mV at all times (provided that $V_{in} = 0$mV), respectively. Fig.4 then captures all the fundamental characteristics of the circuits and accounts of all the performance requirements essential in this study.

An equivalent representation of the block diagram depicted in Fig.4 is given by equation (20) in the form of an augmented plant G. The noise reduction circuit is then converted to the $M\Delta$-loop form considered in the Problem Statement of §3, where

$$M = F_l(G, \mathrm{diag}(F1, F2, K)),$$
$$\Delta = \mathrm{diag}(\Delta_A, \Delta_A, \Delta_P),$$

and $\|\Delta\|_{\infty-ind} < 1$. According to (2), in this particular example, $\Delta \in \mathbf{\Delta}^{rep}$ with $n = 2$, $p_1 = 2$, and $p_2 = 1$. It is important to note that the introduction of a performance block Δ_P, see [10] and [11], allows to transform the robust performance problem into a robust stability

Table 1: Parameter Settings

Parameter Set	#1	#2	#3	#4	#5	#6
$\frac{V_{noise}}{V_{in}}$ (ideal)	0dB	-3dB	-6dB	-9dB	-12dB	-100dB
$\frac{V_{in}}{V_{out}}$ (ideal)	0dB	0dB	0dB	0dB	0dB	0dB
(R_f^1, R_g^1)	(0Ω, ∞Ω)	(995Ω, 1kΩ)	(2.98kΩ, 1kΩ)	(6.94kΩ, 1kΩ)	(14.9kΩ, 1kΩ)	(10GΩ, 1kΩ)
(R_f^2, R_g^2)	(0Ω, ∞Ω)	(0Ω, ∞Ω)	(0Ω, ∞Ω)	(0Ω, ∞Ω)	(0Ω, ∞Ω)	(0Ω, ∞Ω)
K	0	.499	.749	.874	.937	1

$$\begin{bmatrix} y_{\Delta 1} \\ y_{\Delta 2} \\ z \\ y_1 \\ y_2 \\ y_K \end{bmatrix} = \underbrace{\begin{bmatrix} 0 & 0 & 0 & -W_\Delta(s) & 0 & -W_\Delta(s) \\ W_\Delta(s) & 0 & W_\Delta(s)W_d & -W_\Delta(s)A(s) & -W_\Delta(s) & -W_\Delta(s)A(s) \\ W_zA(s) & W_z & W_zW_dA(s) & -W_zA^2(s) & -W_zA(s) & -W_zA^2(s) \\ 1 & 0 & 0 & -A(s) & 0 & -A(s) \\ A(s) & 1 & W_dA(s) & -A^2(s) & -A(s) & -A^2(s) \\ A(s) & 1 & W_dA(s) & -A^2(s) & -A(s) & -A^2(s) \end{bmatrix}}_{G} \begin{bmatrix} u_{\Delta 1} \\ u_{\Delta 2} \\ d \\ u_1 \\ u_2 \\ u_K \end{bmatrix} \tag{20}$$

problem, i.e.,

$$\max_{\substack{\Delta_A \in \mathbf{\Delta}_{LTV}^{1\times 1} \\ \|\Delta_A\|_{\infty-ind}<1}} \|F_u(M, \mathrm{diag}(\Delta_A, \Delta_A))\|_{\infty-ind} \leq 1$$

$$\iff SN_{\mathbf{\Delta}^{rep},\infty}(M) \leq 1.$$

Finally, the system M is converted into discrete-time form (by using bilinear Tustin approximation with a sample-time of 10^{-7} seconds) where its impulse response is truncated after 30 impulses without any significant loss of information. The robust ℓ_∞-stability analysis of the $M\Delta$-loop is therefore possible by way of computing upper and lower bounds for the structured norm $SN_{\mathbf{\Delta}^{rep},\infty}(M)$ using the methodology proposed in §4 and §5.

6.5 Numerical Results

The numerical results are displayed in Tables 2 and 3. The upper and lower bounds for the structured norm of M are computed using Matlab and a nonsmooth optimization toolbox Solvopt, see [9]. For each upper and lower bound value, 20 to 100 local searches are performed and the best cost value is displayed. Each local search is initiated by a randomly chosen starting condition selected over the appropriate feasible set (i.e., (6) or (12)). The results are interpreted below and simulations involving the hardware simulator PSpice, see [13], confirm their correctness.

The results in Table 2 refer to the six parameter settings of Table 1 corresponding to different levels of decrease in the ideal $\frac{V_{noise}}{V_{in}}$ ratio. For each parameter set, the upper and lower bound values are computed by employing Corollaries 4.2 and 5.2. The results in Table 2 allow to assess whether the robust performance objective is satisfied (i.e., whether $\|V_{out}\|_\infty \leq 15$mV when $\|V_{noise}\|_\infty \leq 10$mV and $V_{in} = 0$mV). It is seen that the robust performance criterion is met for the first three parameter settings which impose a less strict low frequency noise reduction requirement. Note that, in all cases selected, it is possible to assess the satisfaction of $SN_{\mathbf{\Delta}^{rep},\infty}(M) \leq 1$ because $1 \notin [\underline{SN}_{\mathbf{Y},\mathbf{N},\infty}(M), \overline{SN}_{\mathbf{D}_\mathbf{a}^{rep},\infty}(M)]$. It is however clear that a very small tightening of the performance objective (say by imposing $\|V_{out}\|_\infty \leq 14.9$mV) would place $1 \in [\underline{SN}_{\mathbf{Y},\mathbf{N},\infty}(M), \overline{SN}_{\mathbf{D}_\mathbf{a}^{rep},\infty}(M)]$ for parameter set #3. The upper bound value $\overline{SN}_{\mathbf{D}_\mathbf{a}^{rep},\infty}(M)$ as well as the size of the gap $\overline{SN}_{\mathbf{D}_\mathbf{a}^{rep},\infty}(M) - \underline{SN}_{\mathbf{Y},\mathbf{N},\infty}(M)$ are seen to increase less rapidly for lower ratios of $\frac{V_{noise}}{V_{in}}$. It is hence reasonable to conjecture that even a very large reduction of the ideal $\frac{V_{noise}}{V_{in}}$ ratio (such as -100dB with parameter set #6) would result in a limited (albeit significant) deterioration of the transient response to V_{noise}. This fact is confirmed by PSpice simulations as illustrated in Fig.5. For completeness, note that the results indicate that $\overline{SN}_{\mathbf{D}_\mathbf{a}^{rep},\infty}(M) - \underline{SN}_{\mathbf{Y},\mathbf{N},\infty}(M) \leq 6\% \cdot \overline{SN}_{\mathbf{D}_\mathbf{a}^{rep},\infty}(M)$.

For the critical parameter set #3, further lower and upper bound values, corresponding to different choices of the sequence **a**, the ordered set **Y**, and the sequence **N** (see Corollaries 4.2 and 5.2), are displayed in Table 3. Similar results could be shown to hold for the other parameter configurations as well. The results of Table 3, labeled UB_i, LB_i, $i = \{1, 2, 3\}$, in terms of the respective bounds, complement those of Table 2 in what follows.

Table 2: Best Upper and Lower Bounds

Parameter Set	$\#1$	$\#2$	$\#3$	$\#4$	$\#5$	$\#6$
Smallest Upper Bound for $SN_{\mathbf{\Delta}^{rep},\infty}(M)$ (i.e., tightest $\overline{SN}_{\mathbf{D}_\mathbf{a}^{rep},\infty}(M)$)	.836	.835	1.000	1.106	1.168	1.237
Largest Lower Bound for $SN_{\mathbf{\Delta}^{rep},\infty}(M)$ (i.e., tightest $\underline{SN}_{\mathbf{Y},\mathbf{N},\infty}(M)$)	.836	.802	.950	1.048	1.103	1.164
Size of the Gap (i.e., $\overline{SN}_{\mathbf{D}_\mathbf{a}^{rep},\infty}(M) - \underline{SN}_{\mathbf{Y},\mathbf{N},\infty}(M)$)	0	.033	.050	.058	.065	.073
Satisfaction of the Robust Performance Objective (i.e., $SN_{\mathbf{\Delta}^{rep},\infty}(M) \leq 1$)	yes	yes	yes	no	no	no

Table 3: Details of the Upper and Lower Bounds of Parameter Set $\#3$

Upper Bounds for $SN_{\mathbf{\Delta}^{rep},\infty}(M)$			Lower Bounds for $SN_{\mathbf{\Delta}^{rep},\infty}(M)$		
$SN_{\mathbf{\Delta}^{ind},\infty}(M) = \rho\Big(\big[\|M^{IJ}\|_1\big]_{\substack{I\in\{1,2,3\}\\J\in\{1,2,3\}}}\Big)$	$\overline{SN}_{\mathbf{D}_\mathbf{a}^{rep},\infty}(M)$		$\underline{SN}_{\mathbf{Y},\mathbf{N},\infty}(M)$		
	$\mathbf{a}=\{0,0\}$	$\mathbf{a}=\{1,0\}$	$\mathbf{Y}=\{\Upsilon_S^{IJ}\}_{\substack{I\in\{1,2\}\\J\in\{1,2\}}}$	$\mathbf{Y}=\{\Upsilon_\pm^{IJ}\}_{\substack{I\in\{1,2\}\\J\in\{1,2\}}}$	
			$\mathbf{N}=\{2,1\}$	$\mathbf{N}=\{4,1\}$	$\mathbf{N}=\{1,1\}$
$\mathrm{UB}_1 = 1.027$	$\mathrm{UB}_2 = 1.006$	$\mathrm{UB}_3 = 1.000$	$\mathrm{LB}_3 = .950$	$\mathrm{LB}_2 = .937$	$\mathrm{LB}_1 = .930$

Although UB_1 is a bound initially developed for $M\Delta$-loop systems subject to independent perturbations, it also delivers a valid upper bound in the presence of repeated perturbations as $\mathbf{\Delta}^{ind} \supset \mathbf{\Delta}^{rep}$. The upper bound UB_3 is clearly the best one as it is the only one that guarantees the required performance. The absolute improvement of the upper bound value that imparts to the augmented approach, as compared to its standard counterpart, is $0.006 = \mathrm{UB}_2 - \mathrm{UB}_3$. The importance of this result is best elucidated by comparing it to the size of the gap: $12.0\% = \frac{\mathrm{UB}_2-\mathrm{UB}_3}{\mathrm{UB}_3-\mathrm{LB}_3}100\%$. A similar comparison between UB_3 and UB_1 yields $54.0\% = \frac{\mathrm{UB}_1-\mathrm{UB}_3}{\mathrm{UB}_3-\mathrm{LB}_3}100\%$. This improvement is obtained with only a very small increase in the overall computational cost. Moreover, while only one augmentation pattern ($\mathbf{a} = \{1,0\}$) allows for a significant improvement of its associated upper bound value, there exists other examples which require more complex choices for $\mathbf{a}$, see [4] for such an example.

As indicated in §5, $N_2 = 1$ in all the three choices of the sequence $\mathbf{N}$ required for lower bound computation. As expected, the computational effort grows significantly with the required precision of the lower bound. Nevertheless, although the absolute difference between LB_3 and LB_2 as well as between LB_3 and LB_1 is only $0.013 = \mathrm{LB}_3 - \mathrm{LB}_2$ and $0.020 = \mathrm{LB}_3 - \mathrm{LB}_1$, respectively, the corresponding relative improvement with respect to the size of the gap is $26.0\% = \frac{\mathrm{LB}_3-\mathrm{LB}_2}{\mathrm{UB}_3-\mathrm{LB}_3}100\%$ and $40.0\% = \frac{\mathrm{LB}_3-\mathrm{UB}_1}{\mathrm{UB}_3-\mathrm{LB}_3}100\%$, respectively. Consequently, while lower bounds involving $\Upsilon_\pm^{IJ}$ may often be advantageous due to their cheaper computational cost, it is certainly worth spending additional computational effort on the computation of a thighter lower bound based on Υ_S^{IJ} if the robustness problem at hand is difficult to assess (i.e., when $1 \in \big[\underline{SN}_{\mathbf{Y},\mathbf{N},\infty}(M), \overline{SN}_{\mathbf{D}_\mathbf{a}^{rep},\infty}(M)\big]$).

Finally, Fig.5 shows the results of the PSpice simulation in which the first panel presents a meaningful benchmark V_{noise} signal, while the remaining ones display the system output V_{out} for the six different parameter choices. The solid lines at ± 15mV are thresholds for the satisfaction of the performance objective. Note that the system with parameter set $\#3$ barely satisfies the objective while the sets $\#4-6$ fails to do so, see Figs.5d to 5g. Also observe that the DC gain of $\frac{V_{noise}}{V_{out}}$ decreases monotonically with respect to the required $\frac{V_{noise}}{V_{in}}$ ratio as expected from the ideal circuit analysis of §6.2.

7 Conclusion

A pair of necessary and sufficient conditions for robust ℓ_∞-stability of systems with *repeated*, linear time-varying, induced ℓ_∞-norm bounded perturbations are presented in this paper. The necessary condition complements the sufficient condition in that it allows to better estimate the value of the structured norm associated with any given robust ℓ_∞-stability problem of the type investigated in this paper. The quality of such estimation is determined by the size of the gap between the corresponding upper and lower bounds.

The proposed theory is shown to be useful for design purposes as confirmed by an application in the field of electronic circuits. Moreover, the simulation results obtained using PSpice, which are comparable to experimental results, further support the conclusion reached.

Future research is intended to compare the theory recently presented in [5] to the one proposed in this paper in the context of the noisy electronic circuit application investigated in §6.

References:

[1] Cadotte, Michalska, Boulet,"A Necessary Condition for Robust ℓ_∞-Stability of Systems with

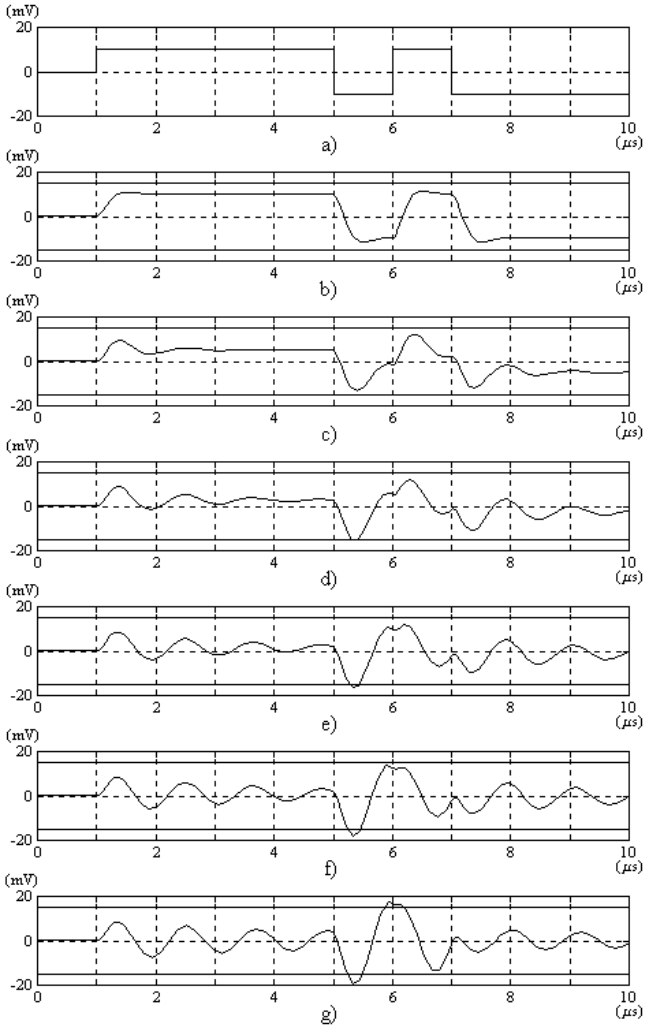

Fig. 5: PSpice simulation results: benchmark V_{noise} signal (top panel) and corresponding V_{out} signals (one for each parameter setting listed in Fig.1).

Repeated Perturbations", Proceedings of the 43^{td} IEEE CDC, pp1352-1357, 2004.

[2] Cadotte, Michalska, Boulet,"Design of a Robust Controller for a Heat Exchanger System with ℓ_∞-Performance Objectives and Repeated Perturbations", *WSEAS Transaction on Systems*, Issue 5, Vol. 3, July 2004, pp2092-2097.

[3] Cadotte, Michalska, Boulet, "Computational Aspects of a Criterion for Robust ℓ_∞-Stability of Systems with Repeated Perturbations", To appear in the Proceedings of the 24^{th} ACC, Robust Stability and Control Session, 2005.

[4] Cadotte, Michalska, Boulet, "An Improved Sufficient Condition for Robust ℓ_∞-Stability of Systems with Repeated Perturbations", To appear in the Proceedings of the 24^{th} ACC, Robust Stability and Control Session, 2005.

[5] Cadotte, Michalska, Boulet, "A Decomposition Approach to Robust ℓ_∞-Stability Analysis of Systems with Repeated Perturbations", Submitted to CDC 2005.

[6] Dahleh, Diaz-Bobillo, *Control of Uncertain Systems: a Linear Programming Approach*, Prentice Hall, 1995.

[7] Fairchild Camera and Instrument Corporation, *Fairchild Linear Op-Amp Data Book*, 1979.

[8] Gayakwad, *Op-Amps and Linear Integrated Circuit Technology*, Prentice-Hall, 1983.

[9] Kappel, Kuntsevich, "An implementation of Shors r-algorithm", *Comput. optim. and applic.*, 15, pp193-205, 2000.

[10] Khammash, "Necessary and sufficient conditions for the robustness of time-varying systems with applications to smapled-data systems", *IEEE TAC*, vol. 38, no. 1, pp49-57, Jan 1993.

[11] Khammash, Pearson, "Performance Robustness of Discrete-Time Systems with Structured Uncertainty", *IEEE TAC*, vol. 36, no. 4, pp398-412, 1991.

[12] Khammash, Pearson, "Analysis and Design for Robust Performance with Structured Uncertainty", *Syst & Contr Lett*, 20, pp179-187, 1993.

[13] Orcad Design Network. (2000) The PSpice Student Version Release 9.1. [Online] Available: http://www.orcad.com/downloads/demo/default.asp

[14] Sedra, Smith, *Microelectronic Circuits*, Oxford press, 4^{th} edition, 1998.

[15] Shamma, "Robust Stability with time-Varying Structured Uncertainty", *IEEE TAC*, vol. 39, no. 4, pp714-724, 1994.

[16] Young, Dahleh, "Robust ℓ_p Stability and Performance", *Syst & Contr Lett*, 26, pp305-312, 1995.

[17] Zhou, Doyle, Glover, *Robust and optimal control*, Prentice-Hall, 1996.